Steady tool wear and its influence on tool geometry in ultra-precision fly cutting

Guoqing Zhang[1], Suet To[2], Xiaoyu Wu[1] and Yan Lou[1]

[1]Guangdong Provincial Key Laboratory of Micro/Nano Optomechatronics Engineering, College of Mechatronics and Control Engineering, Shenzhen University, Shenzhen 518060, China

[2]State Key Laboratory of Ultra-precision Machining Technology, Department of Industrial and Systems Engineering, The Hong Kong Polytechnic University, Hong Kong 00852, China

E-mail: guoqing-zhang@hotmail.com

Abstract

In ultra-precision fly cutting (UPFC), steady tool wear progresses gradually when cutting ductile materials. The steady wear of diamond tools changes the tool geometry, and further affects the topography of the machined surface. In this study, a theoretical and experimental investigation was conducted on the forms of steady tool wear and their influence on the tool geometry in UPFC. The features of steady tool wear in UPFC were investigated, the displacement of the cutting edge under the effects of tool flank wear was modeled, and factors affecting the cutting edge roundness were investigated. The study results indicate the following: (1) The features of steady tool wear in UPFC include crater wear on the rake face, smooth and flat wear on the cutting edge, and flank wear on the tool clearance face. (2) A smooth wear-land on the cutting edge changes the top rake of the cutting tools, whereas flank wear on the tool clearance face affects the clearance angle and roundness of the cutting edge. (3) The maximum width of the tool material loss zone, the nose radius of the original fresh cutting edge, and the arc angle of the wear-land have a certain influence on the nose radius of the worn cutting edge. The results of this study will provide deep insight into steady tool wear and its influence on the tool geometry, which can potentially be used to predict or evaluate the finish of a machined surface under tool steady wear.

Keywords: ultra-precision fly cutting, tool wear, tool geometry, cutting edge roundness

NOMENCLATURE

s_w = swing distance

s_t = step distance

h_t = offset shift of cutting edge

γ = angle of the top rake

ϕ = shift angle

φ = angle between the cross-sectional curves of a fresh clearance face and worn clearance face

δ = clearance angle of the original fresh cutting tool

W_{Max} = the maximum width of tool material loss zone

N_F = nose radius of the original fresh cutting edge

N_W = nose radius of the worn cutting edge

A_W = arc angle of the wear-land

1. Introduction

Tool wear is an unavoidable phenomenon in metal cutting [1]. For conventional cutting, cutting tools are made of high-speed steel, cemented tungsten carbide, cast alloy, and other materials, whereas the materials being cut are limited to ductile materials. According to Shaw and Cookson, tool wear features include tool face wear, cratering, nose wear, wear-land wear, and plastic flow [2]. Stephenson and Agapiou have divided tool wear into three stages: initial wear, steady wear, and severe wear [3]. In evaluating the tool wear level, flank wear was determined by ISO 3685:1993 to be the most commonly used measure of tool wear [4].

Tool wear features in ultra-precision machining differ from those in conventional machining. These differences are attributed to two aspects: First, the cutting tools used in ultra-precision machining are usually made of single crystal diamond, which has super hardness and high thermal conductivity [5]. Second, diamond turnable workpiece materials are broadly used in ultra-precision machining, and not only include ductile materials such as aluminum, copper, and electroless nickel [6-7], but also some brittle materials and hard-to-cut materials [8-9]. Similar to conventional cutting, tool wear features in ultra-precision machining also depend largely on the cutting environment, cutting parameters, tool materials and the work-piece materials being cut. The cutting conditions seriously affect the tool life and tool wear features. For example, Durazo-Cardenas et al. pointed out that the useful life of diamond tools can be extended three-fold through the use of a specific coolant [10]. Cheng et

al. found that cutting heat decreases the cohesion energy of carbon and weakens its bonding, and therefore, the cutting temperature seriously affects diamond tool wear [11]. The cutting parameter is another factor influencing the tool wear features. Palanikumar and Davim explored the cutting parameters that influence the tool wear on the machining of glass fiber-reinforced plastic composites and concluded that the cutting speed has a greater influence on tool flank wear, followed by the feed rate [12]. Similar descriptions were made for other machining process or tool-workpiece materials. Other factors affecting the tool wear features include the tool materials and tool coating. For example, Kılıçkap et al. found that the tool wear is lower when a TiN-coated cutting tool is used in comparison to an uncoated tool for the cutting of particle-reinforced aluminum metal matrix composites [13].

The workpiece materials being cut is a key factor affecting tool wear features in ultra-precision machining. Usually, when cutting brittle materials, the tool wear features are mainly presented as cracks. For example, Zhou et al. indicated that cleavage and micro-chipping appear to be the dominant wear mechanisms under the diamond cutting of optical glass [14-15]. Yan et al. concluded that tool wear features during the diamond cutting of single crystal silicon include two categories: micro-chippings and gradual wear, where the predominant tool wear regime depends on the thickness of the unreformed chip [16]. Another tool wear feature in the diamond cutting of brittle materials is groove formations on the tool clearance face. For example, Zhang et al. found an occurrence of periodical groove wear on the flank face of the cutting tool as diamond turning of reaction-bonded silicon carbide [17]. Li et al. also found similar results in which micro-grooves are formed on the clearance face of diamond tools as nanoscale ductile mode cutting of silicon wafer [18]. However, according to Wada et al. [19] and Oomen & Eisses [20], for a ductile material undergoing diamond cutting such as copper and aluminum, a smooth and flat wear-land is formed, which is quite different from that in diamond cutting of brittle materials.

Ultra-precision fly cutting (UPFC) is a discontinuous cutting process whereby the diamond tool rotates across the spindle while the work-piece is fixed. Song et al. pointed out that the intermittent cutting of ultra-precision fly cutting decreases the contact between the diamond tool and work-piece during the cutting process, which creates superior heat dispersion and therefore suppresses the tool wear occurrence [21]. Yin et al. conducted a comprehensive study on the tool wear features in UPFC, and identified the features of diamond tool wear as being cracks resulting from the impact effects [22]. Zhang et al. found that the tool wear features of UPFC not only include cracks of the cutting edge during the initial tool wear stage, but also wear-land formation during the steady wear stage [23-24].

Cutting tools are the direct executors of the cutting process. Tool wear occurrence has multiple effects on the cutting process, which include increasing the cutting force, enhancing the cutting temperature, and deteriorating the surface quality. During metal cutting, the tool geometry directly affects the surface finish of the machined surface, whereas tool wear changes the tool geometry and further affects the roughness of the machined surface. For example, tool cracks will affect the completion of the cutting edge, whereas craters on the rake face and tool flank wear will change the rake angle and clearance angle of the cutting tool, respectively. Therefore, studies on the effects of steady tool wear and their influence on the tool geometry are meaningful. In the present research, steady tool wear is investigated, the effects of such wear on the tool geometry are explored, and factors affecting the cutting edge roundness are discussed. The present research will provide deep insight into steady tool wear and its relation between tool flank wear and cutting edge roundness in UPFC.

2. Experiments

In this study, a Precitech Freeform 705G (Precitech Inc., USA) five-axis CNC ultra-precision lathe was employed to conduct the cutting experiment. The experimental setup is shown in Figure 1. During the experiment, a diamond tool designed and fabricated by Apex Inc. (UK) was employed to cut the desired flat surface, and the tool geometry parameters are as follows: a radius of 631 μm, top rake angle of -2.5°, and a clearance angle of 15°. The parameters used during the cutting are a cutting depth of 30μm, feed rate of 3.33 mm/s, step distance of 25μm, spindle speed of 75 rps, and swing distance of 28.35 mm. The work-piece material used in this experiment is CuZn30. The total straight cutting distance was around 5,000 m.

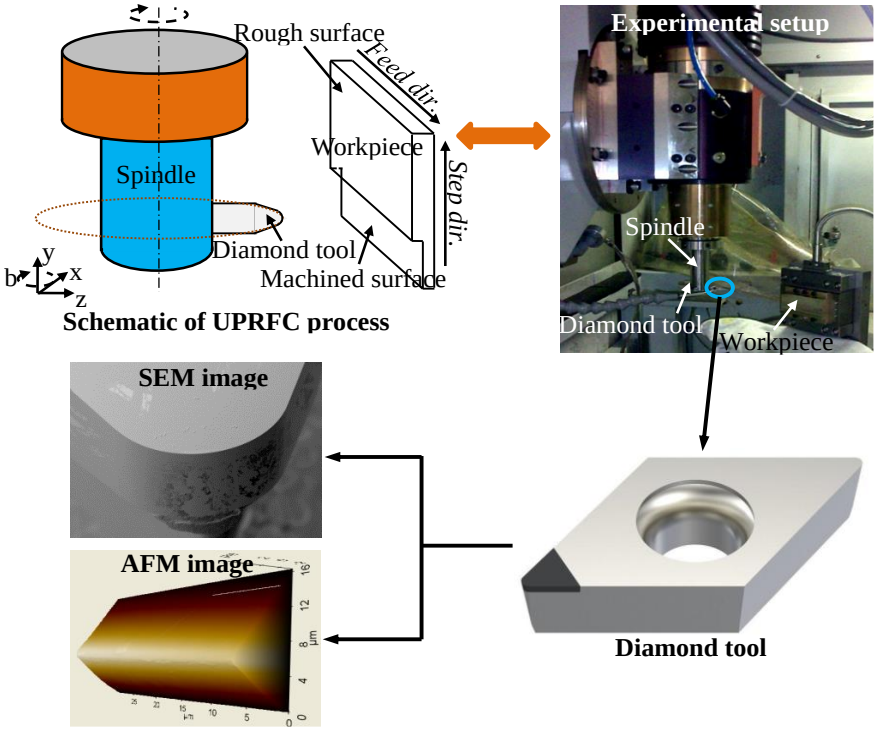

Figure 1. Experimental setup used in this study

After cutting, the diamond tool was dismounted and examined using a Hitachi TM3000 scanning electron microscope (SEM), whereas the cutting edge profile was measured using a Park's XE-70 atomic force microscope (AFM).

3. Results and discussion

3.1 Tool wear features in UPFC

Diamond has excellent mechanical properties, such as an extreme hardness and a low friction coefficient. However, mechanical diamond tool wear is inevitable with an increase in the cutting distance. According to Wada et al. (1980) [15], during the diamond cutting of aluminum alloy, a smooth and flat wear-land was observed on the cutting edge, which increases as the cutting progresses, but hardly influences the roughness of machined surface. During our experiment, a similar phenomenon was observed during the diamond cutting of copper alloy. Figure 2 shows SEM photographs of diamond tool wear after 5,000 m of flat cutting of a CuZn30 alloy, where a smooth and flat wear-land was found on the cutting edge. The wear-land originates from point l_p, shown in Figure 2(c), and terminates at point r_p, shown in Figure 2(b), and is wider at the central point and thinner at both sides, giving it a crescent-shaped profile.

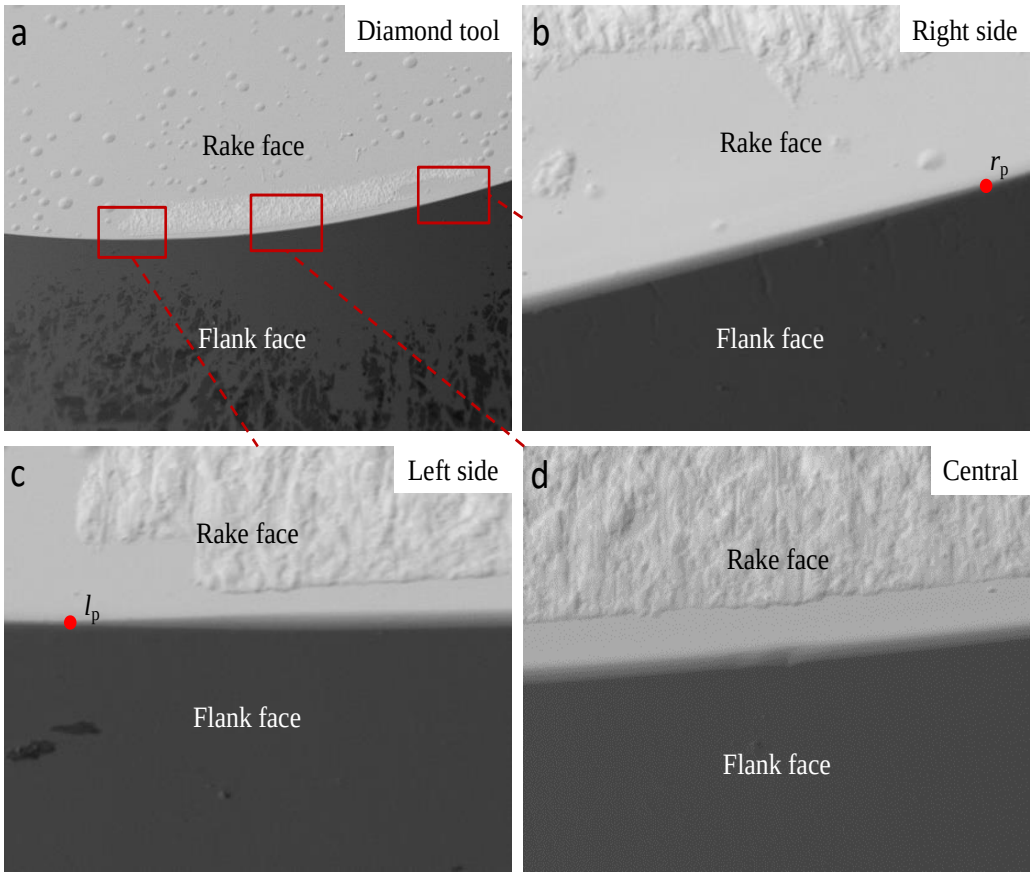

Figure 2. SEM photographs of diamond tool wear after 5,000 m of flat cutting of CuZn30 alloy at magnifications of (a) 500x and (b)-(d) 5000x

Figure 3 shows AFM images of the cutting edge of the worn tool with 5,000 m of flat cutting. It can be seen from Figure 3(a) that a smooth wear-land appears with a width of nearly 1μm, which is the width between the two lines shown in Figure 3(b). Figure 3(c) shows a cross-sectional profile of the cutting edge, which indicates that the wear-land is nearly flat with an angle to the rake face of the diamond tool. In addition, as shown in Figure 3(c), the angle between the rake face and clearance face of the worn tool is about 100°, which differs from the angle when the tool has a fresh cutting edge (i.e., 77.5° based on the geometric parameters of the tool). Because the cross-sectional profile of the tool clearance face is a curve rather than a straight line, and an inflection point t_p exists on the curve, the curve is believed to be formed by tool flank wear on the clearance face.

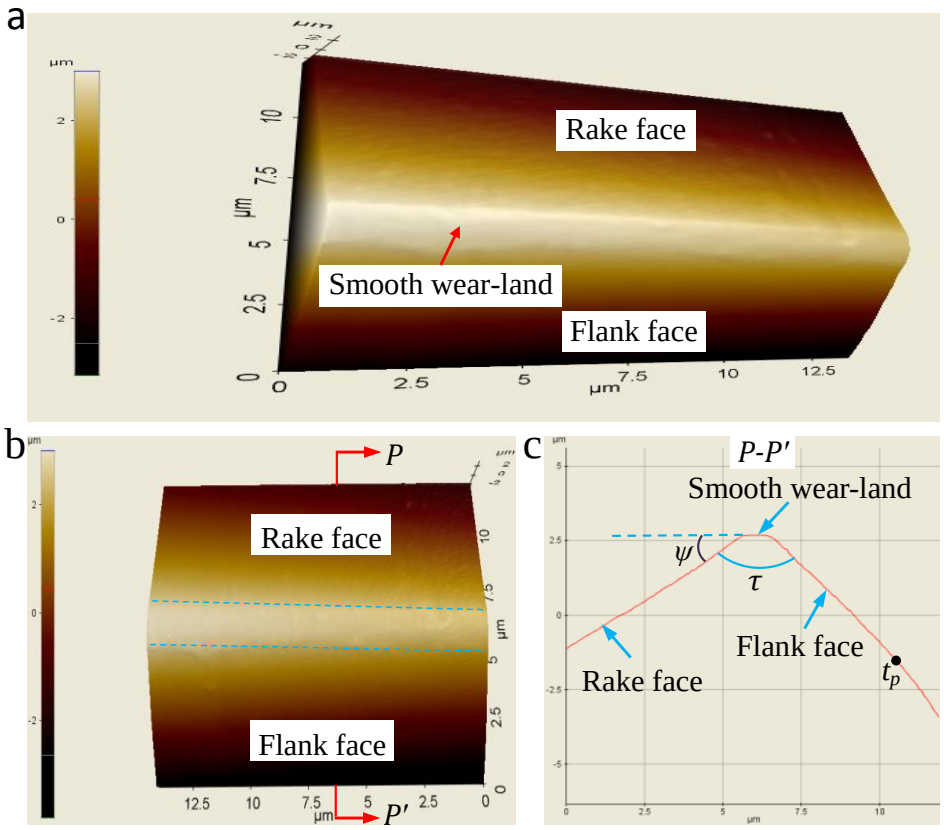

Figure 3. (a)-(b) AFM images of cutting edge and (c) its cross-sectional profile

Figure 4 shows an amplified cross-sectional profile of the cutting edge. As the figure indicates, crater wear is exposed on the rake face of the diamond tool with a maximum depth of σ. Therefore, the steady tool wear in UPFC includes crater wear on the rake face, smooth wear on the cutting edge, and flank wear on the clearance face. Among them, smooth wear can help identify the position of flank wear, e.g., the boundary points and the maximum width of the tool material loss zone (W_{Max}). The occurrence of steady tool wear creates a displacement of the cutting edge and changes the geometric parameters of the tool, thereby affecting the roughness and form accuracy of the machined surface.

In Figure 4, based on the given geometric parameters of the tool, the boundary curve, *bai*, is the cross-sectional boundary curve of the original fresh cutting edge, whereas the solid line is the boundary curve of the worn cutting edge. The triangle Δabc is the tool material loss zone of the diamond tool formed through tool flank wear. The line *ai* is a cross-sectional curve of the rake face of the diamond tool, the line *aj* is the cross-sectional curve of the tool surface, and the line *ak* is the line connecting the center points of the cutting edge and spindle axis. Because *ak* is along the direction of the swing distance (s_w), as shown in Figure 5 (b), the cross-sectional curve of the tool flank wear should be along the cutting direction, that is,

tangent to the tool rotary trajectory. Therefore, the line *bc* should be perpendicular to *ak*. In Figure 4, γ is the angle of the top rake; ϕ is the angle between *aj* and *ak*, called the shift angle; and φ is the angle between the cross-sectional curves of a fresh clearance face and worn clearance face, called the flank wear angle. According to the geometric relation, the flank wear angle $\varphi = \phi + \delta$, where δ is the clearance angle of the original fresh cutting tool.

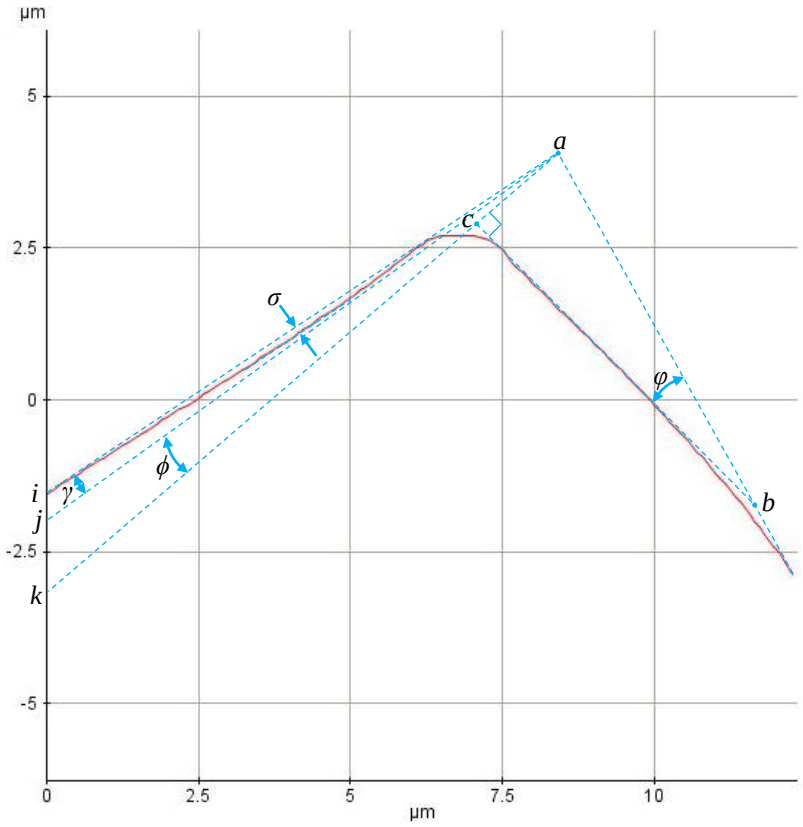

Figure 4. Cross-sectional curve of worn cutting edge (captured using XE-70 AFM, Park)

Figure 5 shows a 3D model of an insert tool and its installation schematic on the tool holder. In Figure 5(b), h_t is the offset shift of the cutting edge center point to the tool holder center line, which can be obtained through a direct measurement, and s_w is the swing distance. According to the geometric relation between the swing distance and offset shift, the following is yielded:

$$\sin\phi = \frac{h_t}{s_w} \tag{1}$$

Based on Eq. (1), shift angle ϕ can be calculated as

$$\phi = \arcsin\left(\frac{h_t}{s_w}\right) \tag{2}$$

In this investigation, h_t = 5 mm and s_w = 28.35 mm, and according to Eq. (2), the shift angle is calculated as ϕ=10.1585°.

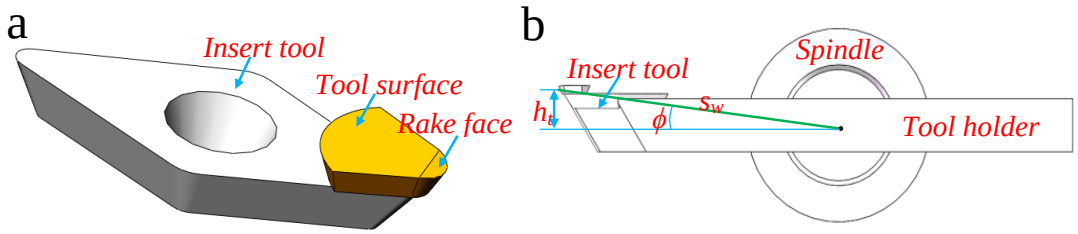

Figure 5. (a)3D model of an insert diamond tool, and (b) its installation schematic on the tool holder

3.2 Identification of the key points of tool material loss zone

The cutting strategy of UPFC makes the participation of the cutting edge in the formation of the surface topography different, for example, certain segments of the cutting edge are used with high frequency, whereas other segments are rarely used. A different usage frequency leads to a different wear rate on the cutting edge segments, and therefore causes different wear-land loss throughout the cutting edge. Based on the discussion above, steady tool wear in UPFC includes flank wear. Similar to the smooth wear, the formation of flank wear makes the cutting edge a crescent-shaped tool material loss zone. In this study, some key points are employed to depict the profile of tool material loss zone: two boundary points of the tool material loss zone and the W_{Max} point. The two boundary points are used to depict the origin and termination of the tool material loss zone, whereas the W_{Max} point is used to point out the location where the displacement of the cutting edge is at maximum.

The surface topography macroscopically affects the position of the key points. In UPFC, a machined surface is generated during cutting tool motion, combining raster motion in the raster direction and fly cutting motion in the feed direction, and therefore, the key points are identified through a synthesis of these two cutting directions. For example, Figure 6 shows an example of sine surface cutting and the key point identification. During surface cutting, the maximum slopes of the surface topography determine the arc window of the cutting edge participating in the cutting. The positive and negative maximum slopes, i.e., t_1 and t_2 in Figure 6 (a), are used to define the two boundary points, l_p and r_p, of the tool material loss zone in Figure 6(b). For the W_{Max} point, it is located at the cutting edge with highest usage. Because a sine surface is symmetrical, W_{Max} should be at the center of the cutting edge, as with point f_p in Figure 6.

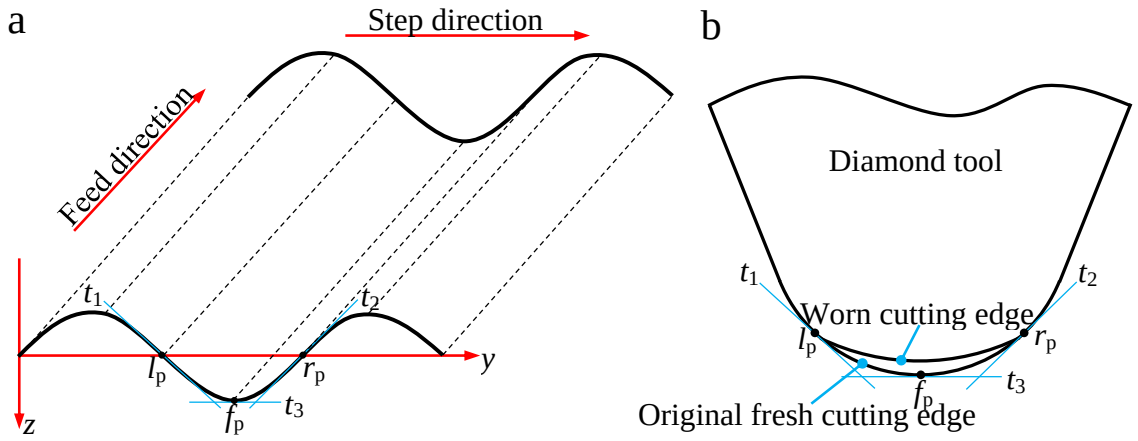

Figure 6. (a) Schematic of sine surface cutting and (b) identification of key points in tool material loss zone

The cutting parameters also affect the position of these key points, which mainly occurs microscopically. Taking an example of flat cutting shown in Figure 7(a), l_p and r_p are the chip boundary points in the step direction, as tool flank wear occurs during the chip formation process, l_p and r_p are also the side boundary points of the tool material loss zone. Therefore, the position of the two boundary points of the tool material loss zone can be identified through a calculation of the cutting parameters. However, to determine W_{Max} herein, its location depends on the chip length. Clearly, W_{Max} is located at the cutting edge segment with the longest cutting distance. As shown in Figure 7(b), the cutting chips in UPFC have a leaf-like morphology. Therefore, at the different points in the step direction (y direction in Figure 7 (b)), the chip length (x direction in Figure 7 (b)) is also different, and the longest chip occurs at point y_0 in the step direction (y-axis). Because a longer chip means a longer cutting distance, herein, y_0 can be used to determine the position of W_{Max}..

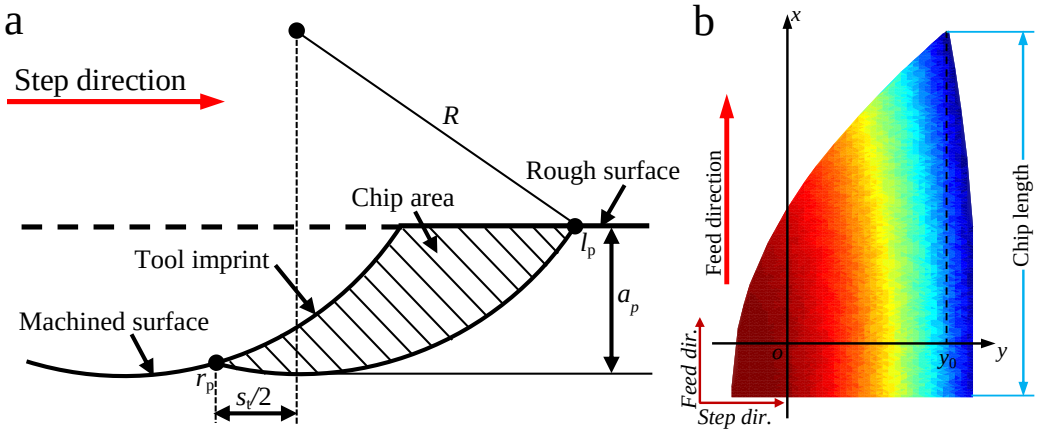

Figure 7. (a) Schematic of chip formation in UPFC, and (b) chip morphology

The positions of the key points are affected by the synthetization of the surface topography and the cutting parameters. For example, for flat-surface cutting, the key points are only affected by the cutting parameters because the maximum slope of the surface topography is always zero. However, for free form surface or other fluctuating surfaces cutting, the positions of the key points are affected not only by the cutting parameters but also by the surface topography. In Figure 2(d), a smooth wear-land can be seen as having the same width, and for simplicity, W_{Max} is defined as the central point of the cutting edge.

3.3 Displacement of cutting edge owing to tool flank wear

3.3.1 Displacement of cutting edge.

The occurrence of steady tool wear causes a displacement of the cutting edge and forms a new cutting edge with different geometric tool parameters. Figure 8 shows a schematic of the displacement of the cutting edge under tool flank wear. As shown in Figure 8(b), suppose that the profile of a worn cutting edge is an arc, and the maximum receding displacement of the worn cutting edge is located at the center of the arc, the worn cutting edge is then found to have a larger nose radius and a change in the arc center.

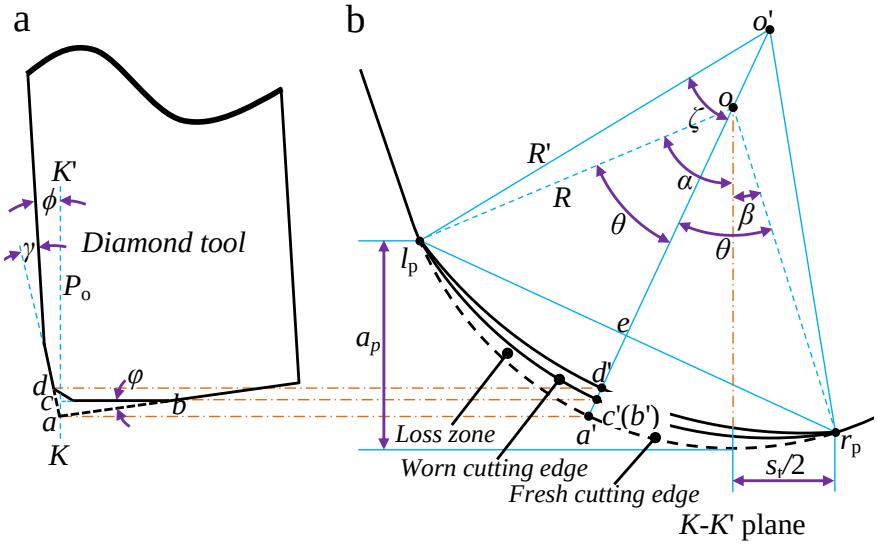

Figure 8. Schematic of receding displacement of worn cutting edge

According to the geometric relation, displacement of the cutting edge ($|\mathrm{ac}|$) can be calculated based on the sine law. In the triangle Δabc shown in Figure 4, $\Delta abc = \varphi$, $|ac|$ is W_{Max} owing to tool flank wear; in addition, $|\mathrm{bc}|$ can be measured using AFM, and therefore

$$\tan\varphi = \tan(\phi + \delta) = \frac{|\mathrm{ac}|}{|\mathrm{bc}|}. \tag{3}$$

From Eq. (3), W_{Max} can be calculated as:

$$W_{Max} = |ac| = |bc| \tan(\phi + \delta). \quad (4)$$

In this investigation, the length of |bc| is measured as 6.4μm, as shown in Figure 4; δ is the clearance angle of the diamond tool, whose value is 15°; and ϕ = 10.1585° is the shift angle. Therefore, based on Eq. (4), W_{Max} can be calculated as 3.0060μm. The calculation results indicate that W_{Max} is large and certainly changes the roundness of the cutting edge, thereby influencing the form accuracy of a machined surface in UPFC.

3.3.2 Tool nose radius of the worn cutting edge

As shown in Figure 8(b), tool flank wear causes a crescent-shaped tool material loss zone, which is wider at the center and thinner at both sides. Suppose that the worn cutting edge originates and terminates at points l_p and r_p respectively, and W_{Max} is located at the center point o′ of the arc.

Based on the geometric relation shown in Figure 8(b) and the given cutting parameters, the following is obtained:

$$\cos\alpha = (R - a_p)/R \cdot \sin\beta = \frac{s_t}{2R} \quad (5)$$

where R is the nose radius of the original fresh cutting edge (N_F), a_p is the depth of the cut, and s_t is the step distance.

From Eq. (5), the two angles α and β are derived as

$$\alpha = \arccos\left(\frac{R - a_p}{R}\right), \quad \beta = \arcsin\left(\frac{s_t}{2R}\right) \quad (6)$$

Therefore, the arc angle of the wear-land (A_W) θ in Figure 8 (b) is expressed as

$$\theta = \frac{\alpha + \beta}{2} \quad (7)$$

In the triangle Δoel_p in Figure 8(b), $|el_p|$ can be expressed as

$$|el_p| = R\sin\theta \quad (8)$$

Similarly, in the triangle $\Delta o'el_p$, $\sin\zeta$ is derived as

$$\sin\zeta = \frac{|el_p|}{R'} = \frac{R\sin\theta}{R'} \quad (9)$$

where R' is the nose radius of the worn cutting edge (N_W).

From Eq. (9), the angle ζ can be solved as

$$\zeta = \arcsin\left(\frac{R\sin\theta}{R'}\right). \quad (10)$$

Because the difference between |a′e| and |b′e| is equal to W_{Max}, the following is yielded:

$$(\mathrm{R}-\mathrm{R}\cos\theta)-(\mathrm{R}'-\mathrm{R}'\cos\zeta)=\mathrm{W}_{\mathrm{Max}}. \quad (11)$$

Submitting Eq. (10) into ζ in Eq. (11) yields

$$\mathrm{R}(1-\cos\theta)-R'\left[1-\cos\left(\arcsin\left(\frac{R\sin\theta}{R'}\right)\right)\right]=\mathrm{W}_{\mathrm{Max}} \quad (12)$$

In Eq. (12), R' can be solved numerically. Based on the given cutting parameters and geometric tool parameters, W_{Max} = 3.0060μm, R = 631 μm, and θ = 0.1647 rad, and therefore, N_{W} (R') can be calculated from Eq. (12) as 969.9601μm.

3.3.3 Relation between nose radius of the worn cutting edge and wear-land parameters

Equation (12) indicates the relation between the nose radius of the worn cutting edge (N_{W}) and the wear-land parameters. From Eq. (12), it can be found that the N_{W} (R') has a relation with the maximum width of the tool material loss zone (W_{Max}), the nose radius of original fresh cutting edge (N_{F}) (R), and the arc angle of the wear-land (A_{W}) (θ). Figure 9 shows a curve of the N_{W} with respect to W_{Max}, and it can be seen that, with an increase in W_{Max}, N_{W} gently increases first. However, as W_{Max} is larger than a certain value (around 8μm herein), N_{W} increases sharply to infinity, and then directly decreases to a negative value, which means the curvature of the cutting edge has been transited from positive to negative. Because the curvature of the cutting edge cannot theoretically be negative, the descending segment of the curve in Figure 9 is not meaningful. Therefore, it is concluded that W_{Max} can seriously affect N_{W}, particularly when larger than a certain value, which depends on the N_{F} and A_{W}. As W_{Max} is 3.0060 μm in this paper, as shown in Figure 9(b), N_{W} is about 970μm, which matches the calculated result (969.9601μm).

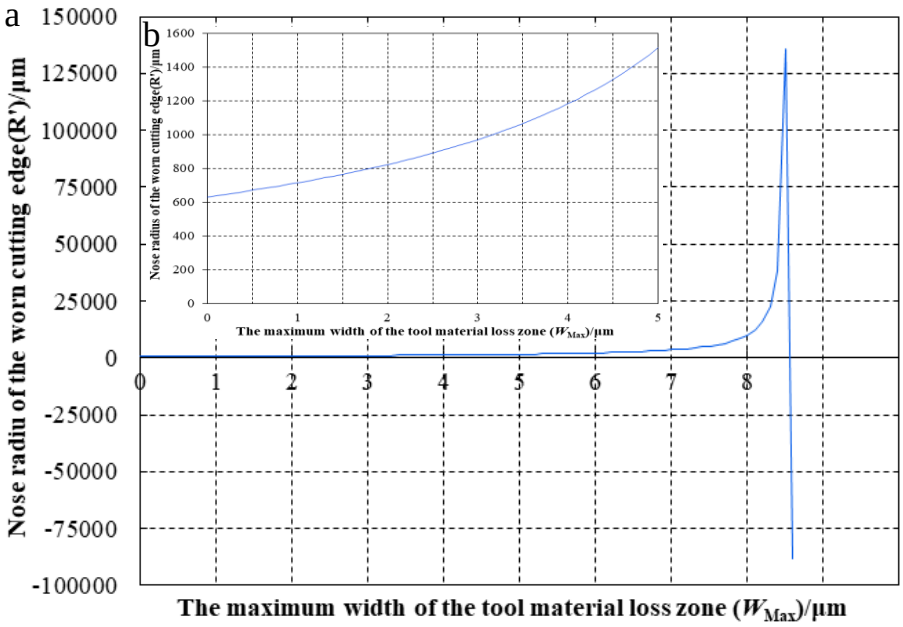

Figure 9. Relation curve between the nose radius of the worn cutting edge (N_W) and the maximum width of the tool material loss zone (W_{Max})

From Eq. (12), the nose radius of the worn cutting edge (N_W) also has a certain relation with the nose radius of the original fresh cutting edge (N_F). This indicates that, if the N_F is chosen differently, after steady tool wear occurs with the same W_{Max} and A_W, the N_W will also differ. The relation curve between N_W and N_F is shown in Figure 10, and it can be seen that N_W and N_F have a nearly linear relation. As N_F changes within a commonly used range of 0.1 to 2.5 mm, N_W increases at an approximately linear rate under the given W_{Max} and A_W. This approximately linear relation can be potentially used to predict N_W of a group of tools cutting the same work-piece material using the same cutting parameters and at a similar cutting distance.

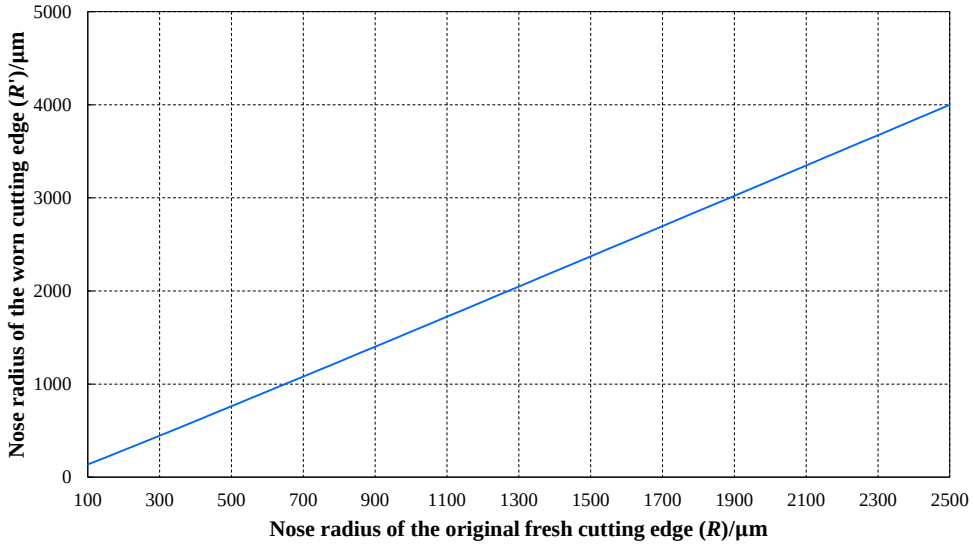

Figure 10. Relation curve between the nose radius of the worn cutting edge (N_W) and the nose radius of original fresh cutting edge (N_F)

Similarly, the arc angle of the wear-land (A_W) also has a certain effect on the nose radius of the worn cutting edge (N_W). As the maximum width of the tool material loss zone (W_{Max}) and the original fresh cutting edge (N_F) are constant, based on Eq. (12), A_W has a complex relation with N_W. Figure 11 shows the relation curve between them, in which, with an increase in A_W, it can be seen that the curve of N_W drops rapidly when the A_W is less than a certain value (0.0978 rad herein) and then gently declines, this certain value depends on N_F and W_{Max}. It can also be seen from Figure 11 that, as A_W declines to a certain value (around 0.0977 rad from Figure 11 (a)), N_W increases to infinity, which means the cutting edge is nearly a

straight line. Therefore, A_W cannot be less than this particular value (around 0.0977 rad) for the given wear-land parameters. In this paper, according to the cutting parameters provided and Eq. (7), A_W was calculated as 0.1647 rad, herein, the N_W is found to be around 970μm, as shown in Figure 11(b), which agrees well with the calculated result (969.9601μm) in this paper.

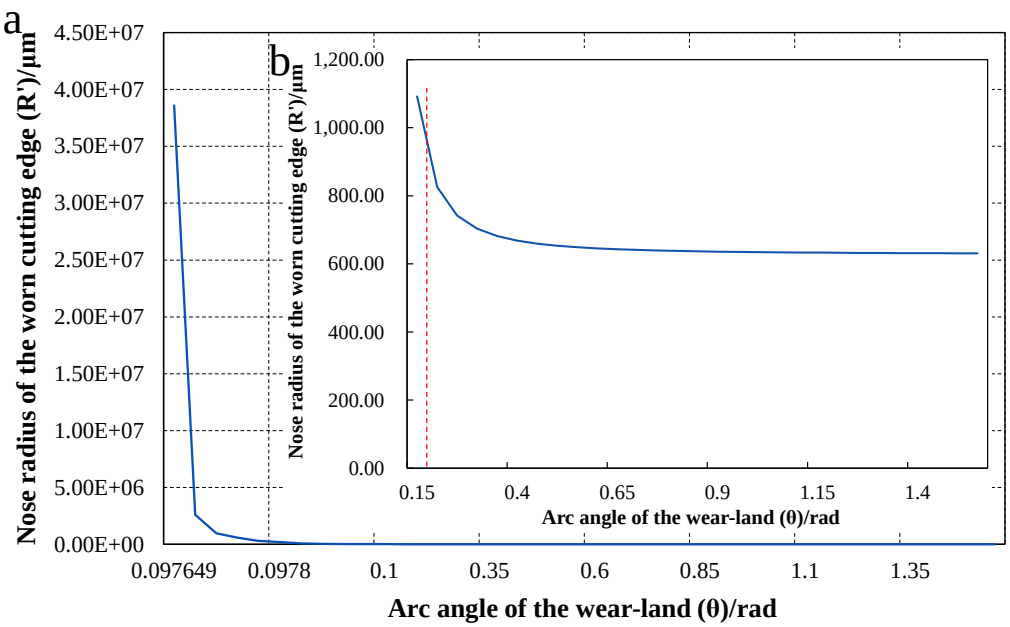

Figure 11. Relation curve between the nose radius of the worn cutting edge (N_W) and the arc angle of the wear-land (A_W)

Because W_{Max} is closely related to the cutting distance, A_W depends on the cutting parameters, and N_F is different for the different cutting tools, their relations to N_W can be used to predict the steady wear level of a cutting tool with similar cutting distance, cutting parameters, or tool nose radius.

4. Conclusions

In the present research, steady tool wear and its influence on the geometry of a cutting tool during ultra-precision fly cutting (UPFC) were investigated. The nose radius of the worn cutting edge (N_W) and its relations to the maximum width of the tool material loss zone (W_{Max}), the nose radius of the original fresh cutting edge (N_F), and the arc angle of the wear-land (A_W) were modeled. The specific conclusions drawn from the present research are as follows:

(i) Steady tool wear when UPFC ductile materials include crater wear on the rake face, smooth wear on the cutting edge, and flank wear on the clearance face. Flank wear on the clearance face changes the flank angle and nose radius of cutting tools.

(ii) The steady wear when UPFC ductile materials is quite smooth; however, it causes the cutting edge to recede by 3μm under the given cutting parameters and cutting conditions, which will affect the roughness and form accuracy of the machined surface.

(iii) The profile and range of tool wear-land are influenced by the topography of the surface being machined at the macroscopic level and by the cutting parameters at the microscopic level.

(iv) Displacement of the cutting edge owing to tool flank wear will lead to an increase in N_W, which increases with a raise in W_{Max} and N_F, and decreases with the growth of A_W.

Acknowledgements

This work was supported by the National Natural Science Foundation of China under Grant (51505297, 51575360 and 51675347); the Natural Science Foundation of Guangdong Province under Grant (2017A030313295 and 2014A030310261); the Shenzhen Science and Technology Program under Grant (JCYJ20160422170026058); and the Shenzhen Peacock Technology Innovation Project under Grant (KQJSCX20170727101318462).

References

[1]. Zhang Y, Zhou Z, Lv Y, Wang J, Shao L, Iqbal A (2013) Wear behavior of natural diamond tool in cutting tungsten-based alloy. International Journal of Advanced Manufacturing Tech nology 69(1-4):329-335

[2]. Shaw MC, Cookson JO (2005) Metal cutting principles. Oxford University Press.

[3]. Stephenson DA, Agapiou JS (2006) Metal cutting theory and practice, Second edition. Tayl or&Francis Group CRC press.

[4]. ISO 3685-1993(E) (1993) Tool life testing with single point turning tools. ISO standard.

[5]. Yazu S, Nakai T (1991) Tool application of diamond and cbn. Materials Science Monographs 73:37-41

[6]. Cheung CF, Lee WB (2002) Prediction of the Effect of Tool Interference on Surface Gener ation in Single-Point Diamond Turning. International Journal of Advanced Manufacturing Technology 19(4):245-252

[7]. Tian F, Yin Z, Li S (2016) A novel long range fast tool servo for diamond turning. Internati

onal Journal of Advanced Manufacturing Technology 86(5-8):1-8

[8]. Mir A, Luo X, Cheng K, Cox A (2018) Investigation of influence of tool rake angle in singl e point diamond turning of silicon. International Journal of Advanced Manufacturing Tech nology (5-8):2343-2355

[9]. Zhang Z, Yan J, Kuriyagawa T (2011) Study on tool wear characteristics in diamond turning of reaction-bonded silicon carbide. International Journal of Advanced Manufacturing Technology 57(1-4):117-125

[10]. Durazo-Cardenas I, Shore P, Luo X, Jacklin T, Impey SA, Cox A (2007) 3d characteriza tion of tool wear whilst diamond turning silicon. Wear 262:340-349

[11]. Cheng K, Luo X, Ward R, Holt R (2003) Modeling and simulation of the tool wear in n anometric cutting. Wear 255:1427-1432

[12]. Palanikumar K, Davim JP (2009) Assessment of some factors influencing tool wear on t he machining of glass fibre-reinforced plastics by coated cemented carbide tools. Journal o f materials processing technology 209:511-519

[13]. Kılıçkap E, Çakır O, Aksoy M, İnan A (2005) Study of tool wear and surface roughness in machining of homogenised sic-p reinforced aluminium metal matrix composite. Journal of Materials Processing Technology 164:862-867

[14]. Zhou M, Ngoi BKA, Yusoff MN, Wang XJ (2006) Tool wear and surface finish in diam ond cutting of optical glass. Journal of Materials Processing Technology 174:29-33

[15]. Jia P, Zhou M (2012) Tool wear and its effect on surface roughness in diamond cutting of glass soda-lime. Chinese Journal of Mechanical Engineering 25:1224-1230

[16]. Yan J, Syoji K, Tamaki J (2003) Some observations on the wear of diamond tools in ultr a-precision cutting of single-crystal silicon. Wear 255:1380-1387

[17]. Zhang Z, Yan J, Kuriyagawa T (2011) Study on tool wear characteristics in diamond tu rning of reaction-bonded silicon carbide. International Journal of Advanced Manufacturing Technology 57:117-125

[18]. Li XP, He T, Rahman M (2005) Tool wear characteristics and their effects on nanoscale ductile mode cutting of silicon wafer. Wear 259:1207-1214

[19]. Wada R, Kodama H, Nakamura K, Mizutani Y, Shimura Y, Takenaka N (1980) Wear characteristics of single crystal diamond tool. CIRP Annals - Manufacturing Technology 29:47-52

[20]. Oomen JM, Eisses J (1992) Wear of monocrystalline diamond tools during ultraprecisio n machining of nonferrous metals. Precision Engineering 14:206-218

[21]. Song YC, Nezu K, Park CH, Moriwaki T (2009) Tool wear control in single-crystal

diamond cutting of steel by using the ultra-intermittent cutting method. International Journal of Machine Tools & Manufacture 49:339-343

[22]. Yin ZQ, To S, Lee WB (2009) Wear characteristics of diamond tool in ultraprecision raster milling. International Journal of Advanced Manufacturing Technology 44:638-647

[23]. Zhang G, To S, Zhang S (2016) Relationships of tool wear characteristics to cutting mechanics, chip formation, and surface quality in ultra-precision fly cutting. International Journal of Advanced Manufacturing Technology 83:133-144

[24]. Zhang G, To S, Zhang S (2016) Evaluation for tool flank wear and its influences on surface roughness in ultra-precision fly cutting. International Journal of Mechanical Sciences 118:125-134